APPLIED PHYSICS LETTERS **100**, 253108 (2012)

Controlled doping of graphene using ultraviolet irradiation

Zhengtang Luo,[1] Nicholas J. Pinto,[2] Yarely Davila,[2] and A. T. Charlie Johnson[3,a)]
[1]*Department of Chemical and Biomolecular Engineering, The Hong Kong University of Science and Technology, Clear Water Bay, Hong Kong, China*
[2]*Department of Physics and Electronics, University of Puerto Rico at Humacao, Humacao, Puerto Rico 00792, USA*
[3]*Department of Physics and Astronomy, University of Pennsylvania, Philadelphia, Pennsylvania 19104-6396, USA*

(Received 27 February 2012; accepted 4 June 2012; published online 20 June 2012)

The electronic properties of graphene are tunable via doping, making it attractive in low dimensional organic electronics. Common methods of doping graphene, however, adversely affect charge mobility and degrade device performance. We demonstrate a facile shadow mask technique of defining electrodes on graphene grown by chemical vapor deposition (CVD) thereby eliminating the use of detrimental chemicals needed in the corresponding lithographic process. Further, we report on the controlled, effective, and reversible doping of graphene via ultraviolet (UV) irradiation with minimal impact on charge mobility. The change in charge concentration saturates at $\sim 2 \times 10^{12}\,\text{cm}^{-2}$ and the quantum yield is $\sim 10^{-5}$ e/photon upon initial UV exposure. This simple and controlled strategy opens the possibility of doping wafer-size CVD graphene for diverse applications. © *2012 American Institute of Physics*. [http://dx.doi.org/10.1063/1.4729828]

The exceptionally high room temperature carrier mobility of graphene offers potential for device applications that have attracted enormous interest in the research community. Various methods have been used to tailor the graphene properties for desired applications, including chemical doping,[1–3] electrochemical doping,[4] and metal contact doping,[5] and other metals including bismuth and antimony.[6] Reports of conventional chemical doping have relied on strong dopants such as potassium[7] and ammonia gas,[2] which act as strongly charged impurities and consequently degrade the carrier mobility. It is highly desirable therefore to develop alternative approaches to controlled doping of graphene nanostructures that avoid these effects. Here, we realize controlled doping of graphene grown by chemical vapor deposition (CVD) by exposure to ultraviolet (UV) radiation with minimal impact on the material's electronic properties, including carrier mobility.

Figure 1(a) is an optical micrograph of a graphene film synthesized by CVD and then transferred onto 300 nm oxide thickness silicon substrate, using a method reported previously.[8,9] A typical Raman spectrum (Fig. 1(b)) shows a symmetric and high intensity 2D band at $\sim 2695\,\text{cm}^{-1}$, characteristic of single layer graphene.[10] Moreover, the D band ($\sim 1345\,\text{cm}^{-1}$) intensity, whose relative strength is proportional to disorder in graphitic materials, is only 0%–5% of the G peak ($\sim 1590\,\text{cm}^{-1}$) intensity, indicating that the graphene material used here is of high quality, as confirmed by electron transport data presented below.

By accurately controlling the growth time and/or position in the furnace, we grew single crystal hexagonal flakes of graphene in random locations with desired size (up to 50 μm) and areal density.[11] In order to avoid sample contamination from polymeric resists,[12] contacts were then fabricated to single flakes using a mechanical shadow mask, as follows. A transmission electron microscopy (TEM) sample grid (Electron Microscopy Sciences TVM-Cu, with 150, 200, 300, 400 mesh holes) was carefully placed over a

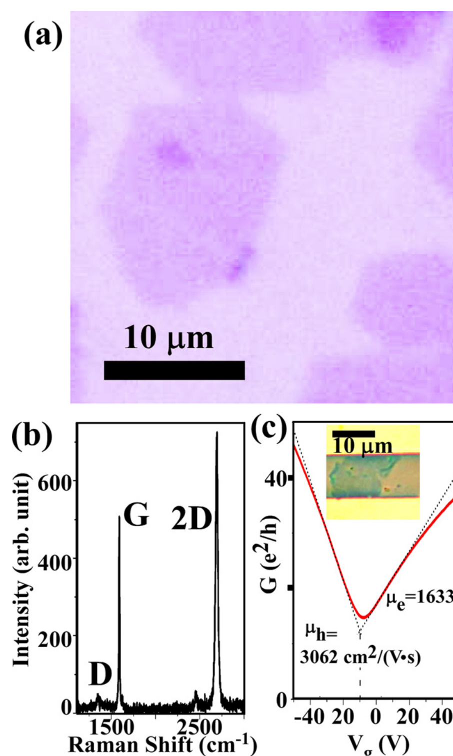

FIG. 1. Graphene synthesized by CVD. (a) Optical micrograph of graphene flakes transferred onto a silicon wafer with a 300 nm-thick oxide. (b) Typical Raman spectrum measured on a graphene flake. (c) Conductance-gate voltage characteristic of a single flake sample measured using the substrate as a backgate. The carrier mobility of 2000–3000 cm^2/V-s is comparable to that for exfoliated graphene on a similar substrate. Inset: Optical micrograph of a graphene flake contacted by two gold electrodes using shadow mask method.

a)Author to whom correspondence should be addressed. Electronic mail: cjohnson@physics.upenn.edu.

 © 2012 American Institute of Physics

Downloaded 27 Jun 2012 to 130.91.117.41. Redistribution subject to AIP license or copyright; see http://apl.aip.org/about/rights_and_permissions

graphene flake and slightly fixed to the substrate with silver paint. Electrical contacts (100 nm thick Ag or Au) were then evaporated through the TEM grid shadow mask onto the substrate, and the TEM grid was removed to yield metal electrodes in contact with a pre-selected graphene flake. The electrical properties of the flake could be measured in a three-terminal geometry, with the degenerately doped silicon substrate used as a backgate. The measured device transfer characteristics and mobility (see below) indicate that this method of contact fabrication leaves the graphene in better condition than when conventional lithographic methods are used. The inset to Fig. 1(c) shows a graphene flake that was contacted by two gold electrodes in the manner just described. Future experiments will be directed towards achieving yet more accurate control over the graphene flake size and density to increase the yield of high-quality graphene devices produced with this method.

Figure 1(c) is a plot of the conductance G, expressed in units of the conductance quantum e^2/h, versus gate voltage (V_g) for an as-fabricated CVD graphene device measured under vaccum of 10 mTorr. The G-V_g plot shows a typical "V" shape that is characteristic of graphene, with enhanced current in the *hole*-branch compared to that in the *electron*-branch; similar observations on exfoliated graphene were attributed to different contact resistances for the different carrier types.[13] From its minimum (the Dirac point), the conductance increases linearly with V_g for both carrier polarities, indicating that the mobility is independent of carrier concentration and type, in agreement with measurements of exfoliated graphene[14] as well for graphene produced by CVD.[8,15] At gate voltages further from the Dirac point, G(V_g) shows a sub-linear growth, most likely due to the presence of charged impurities or water underneath the graphene flake.[7] Here, the minimum conductivity (G_{min}) and corresponding gate voltage ($V_{g,min}$) were obtained by extrapolating the linear portion of the G-V_g curves. As shown in Fig. 1(c), G_{min} shows a similar value as exfoliated graphene, of multiple of $4e^2/h$, a well-established universal value for ideal graphene. The fact that $V_{g,min}$ exhibits a non-zero value, along with the fact that the width of the minimum conductivity region in V_g is broad, indicates the existence of disorder and presence of charge impurities.[1]

A key aspect of the data is that the room temperature hole and electron mobility are found to be large, 3060 and 1630 cm^2/V-s, respectively, comparable to values for exfoliated graphene (2000–10 000 cm^2/V-s) measured by us and others.[16,17] The Raman and electron transport data provide strong evidence that the CVD graphene samples produced with our method are of high structural and electronic quality.

Figure 2(a) shows G-V_g plots for an as-prepared graphene device and for the same device at four different carrier concentration (doping) levels induced by irradiation with UV light ($\lambda = 365$ nm) for progressively longer times, all measured at 295 K and 10 mTorr. Upon UV-doping, the following features are seen: (1) the Dirac point back gate voltage, $V_{g,\ min}$, gradually shifts to more negative voltage, indicative of *n*-type doping due to illumination; (2) the shift of the G-V_g characteristic is rigid, with almost no change in the minimum conductance or the width of the V-shaped curve. We find that the electron mobility is unchanged or

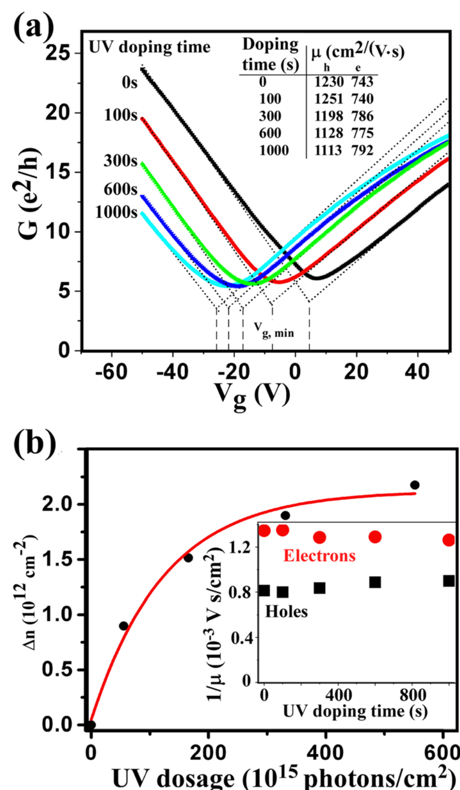

FIG. 2. UV doping of CVD graphene. (a) The conductance (G) versus gate voltage (V_g) curves for different doping time, measured at room temperature and a pressure of 10^{-2} Torr. Dotted lines are linear fits used to obtain the carrier mobilities shown in the inset table. (b) Injected carrier concentrations obtained in (a) as a function of photon flux and an exponential fit. Inset shows the plot of inverse carrier mobilities as a function of doping time.

even increased while the hole mobility is slightly decreased (both effects are no more than 5% in size); (3) as seen in Fig. 2(b), the UV doping effect shows a saturation behavior at $\sim 2 \times 10^{12}$ e/cm^2 with a quantum yield of $\sim 10^{-5}$ e/photon upon initial illumination.

These observations show that the carrier addition (doping) induced by UV irradiation leads to no significant change in the carrier scattering rate. The physical rationale for such a phenomenon remains unclear. The observation is similar to what was found for graphene subject to chemical gating by exposure to gas vapors[17,18] and differs dramatically from the effect of alkali atom dopants like potassium, where the shift in the Dirac point is accompanied by a sharp decrease in mobility.[7] The potassium data were well explained by a picture where ionized potassium ions act as screened Coulomb scattering sites. Theory predicts a conductance that varies linearly with V_g, where the slope is proportional to the carrier mobility, which is inversely proportional to the charged impurity density, n_{imp}: $1/\mu \propto n_{imp}$ for both hole and electron carriers.[19] This behavior is *not* characteristic of our data, as seen in the inset in Fig. 2(b): $1/\mu$ is essentially constant with doping time, which reflects a change in the carrier density.

The UV doping effect described here is stable under vacuum conditions, slowly reverses when the sample is returned to ambient (timescale of days), and reverses within tens of minutes at elevated temperatures in ambient. The reversible nature of the doping is reflected in Fig. 3, which shows the G(V_g) characteristics for a CVD graphene device

Downloaded 27 Jun 2012 to 130.91.117.41. Redistribution subject to AIP license or copyright; see http://apl.aip.org/about/rights_and_permissions

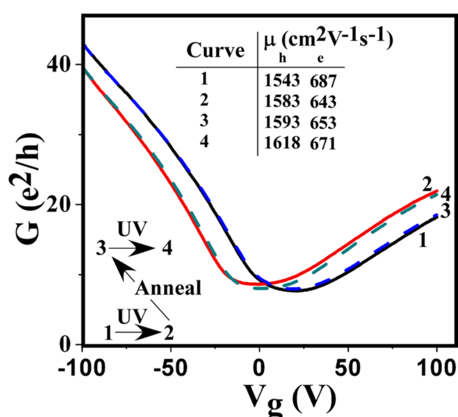

FIG. 3. UV doping of CVD-graphene is fully reversible. The plot shows conductance (G) versus gate voltage (V_g) curves for the same sample when (1) as-made device (solid blue line), (2) after 16 min of UV-doping (solid red line) and (3) after annealing in air at 80 °C for 45 min (black dashed line), and (4) re-doped by exposure to UV for 16 min (dashed green line). All measurements are done at 295 K at a pressure of 10 mTorr.

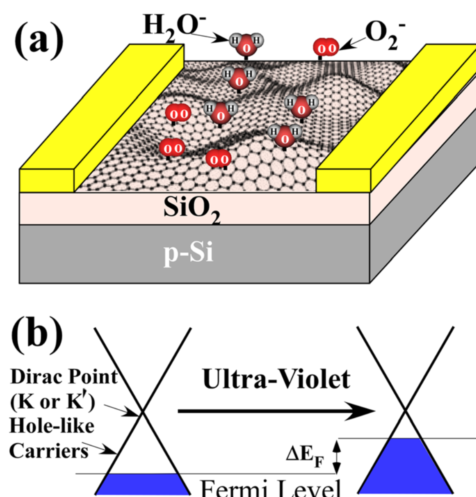

FIG. 4. (a) Schematic of a graphene device showing electron-trapping species adsorbed on the graphene surface (b) The linear dispersion relation characteristic of graphene. Upon UV irradiation, photo-generated holes recombine with the negatively charged adsorbates at the surface and consequently shift the Fermi level to higher energy.

that is first doped by UV irradiation for 16 min, regenerated by annealing at 80 °C for 45 min in ambient, and then UV-doped a second time for 16 min (see inset). All measurements are done at 295 K and 10 mTorr. We observe that curves 1 and 3 are almost identical, indicating that the electronic transport properties of as-fabricated CVD-graphene device are fully recovered by annealing. Re-exposure to UV-irradiation at the same condition leads to a $G(V_g)$ trace identical to that measured after the first doping step (curves 2 and 4). This provides strong evidence that the UV-doping is reversible and reproducible with no significant damage or "poisoning" effect.

The exact doping-de-doping mechanism is not clear at present. Recent work[20–23] has shown that charge transfer at the substrate interface plays a vital role in the electronic properties of graphene and that this can be tuned by varying the identity of molecules between the silicon substrate and the graphene channel. A shift of the Fermi level, ΔE_F, of -0.35 to 0.09 eV was reported by surface treatment of the substrate, including adding a hydrophobic monolayer between graphene and the silicon substrate,[20] modifying the substrate with silane or polymer molecules with amine or fluorine-containing groups,[21] or trapping water molecular between graphene and the silicon substrate.[23] In the present work, the gradual shift of Dirac point (i.e., $V_{g,\,min}$) to negative gate voltage upon illumination suggests the influence of a similar change in surface charge on the electronic properties of the graphene. Electron trapping adsorbate groups[21,23] on the graphene surface or graphene-substrate interface (possibly O_2- or H_2O- derived), a natural consequence of exposure to air, would typically lead to *p*-type doping as is commonly observed for graphene FET devices, including those presented here. Upon UV exposure, an electron-hole pair is generated that liberates the adsorbates via hole recombination (e.g., $h^+ + O_2- \rightarrow O_2$ (gas)) on both sides of CVD graphene, releasing electrons that then contribute toward *n*-doping (Figures 4(a) and 4(b)). Since this process, unlike chemical doping, does not significantly modify the structure of graphene, one expects only limited effect on the carrier mobility, consistent with our observations.

In conclusion, we have demonstrated a facile shadow mask technique to define electrodes on CVD graphene and report a method to controllably change the carrier concentration in the graphene via UV irradiation. Unlike other doping techniques with strong dopant atoms or molecules, this method was found to have minimal impact on the material's electronic properties other than the carrier concentration, evidenced by the observation of minimal variation in carrier mobility during the doping and de-doping process. This simple and controlled doping strategy allows tuning the electric properties of wafer-size CVD graphene in defined areas through the use of light absorbing masks and it opens the possibility of diverse applications.

Z.L. and A.T.C.J. were supported by the National Science Foundation through grant DMR-0805136. N.J.P acknowledges support from NSF DMR under grants PREM-0934195 and RUI-0965023. Y.D. gratefully acknowledges the support of the REU program of the Laboratory for Research on the Structure of Matter (NSF REU Site Grant DMR-1062638).

[1]J.-H. Chen, C. Jang, S. Xiao, M. Ishigami, and M. S. Fuhrer, Nat. Nanotechnol. **3**, 206–209 (2008).
[2]X. Wang, X. Li, L. Zhang, Y. Yoon, P. K. Weber, H. Wang, J. Guo, and H. Dai, Science **324**, 768–771 (2009).
[3]M. Kim, N. S. Safron, C. Huang, M. S. Arnold, and P. Gopalan, Nano Lett. **12**, 182–187 (2012).
[4]A. Das, S. Pisana, B. Chakraborty, S. Piscanec, S. K. Saha, U. V. Waghmare, K. S. Novoselov, H. R. Krishnamurthy, A. K. Geim, A. C. Ferrari *et al.*, Nat. Nanotechnol. **3**, 210–215 (2008).
[5]G. Giovannetti, P. A. Khomyakov, G. Brocks, V. M. Karpan, J. van den Brink, and P. J. Kelly, Phys. Rev. Lett. **101**, 026803 (2008).
[6]I. Gierz, C. Riedl, U. Starke, C. R. Ast, and K. Kern, Nano Lett. **8**, 4603–4607 (2008).
[7]J. H. Chen, C. Jang, M. S. Fuhrer, E. D. Williams, and M. Ishigami, Nat. Phys. **4**, 377–381 (2008).
[8]K. S. Kim, Y. Zhao, H. Jang, S. Y. Lee, J. M. Kim, K. S. Kim, J.-H. Ahn, P. Kim, J.-Y. Choi, and B. H. Hong, Nature **457**, 706–710 (2009).
[9]H. Cao, Q. Yu, L. A. Jauregui, J. C. Tian, W. Wu, Z. Liu, R. Jalilian, D. K. Benjamin, Z. Jiang, J. Y. Bao *et al.*, Appl. Phys. Lett. **96**, 122106 (2010); X. Li, W. Cai, J. An, S. Kim, J. Nah, D. Yang, R. Piner, A. Velamakanni, I. Jung, E. Tutuc *et al.*, Science **324**, 1312–1314 (2009); Z. Luo, Y. Lu,

Downloaded 27 Jun 2012 to 130.91.117.41. Redistribution subject to AIP license or copyright; see http://apl.aip.org/about/rights_and_permissions

D. W. Singer, M. E. Berck, L. A. Somers, B. R. Goldsmith, and A. T. C. Johnson, Chem. Mater. **23**, 1441–1447 (2011).
[10]A. C. Ferrari, J. C. Meyer, V. Scardaci, C. Casiraghi, M. Lazzeri, F. Mauri, S. Piscanec, D. Jiang, K. S. Novoselov, S. Roth *et al*., Phys. Rev. Lett. **97**, 187401 (2006).
[11]Z. Luo, S. Kim, N. Kawamoto, A. M. Rappe, and A. T. Charlie Johnson, ACS Nano **11**, 9154–9160 (2011).
[12]S. M. Khamis, R. A. Jones, and A. T. Charlie Johnson, AIP Adv. **1**, 022106 (2011).
[13]F. Xia, V. Perebeinos, Y.-M. Lin, Y. Wu, and P. Avouris, Nat. Nanotechnol. **6**, 179–184 (2011).
[14]K. S. Novoselov, A. K. Geim, S. V. Morozov, D. Jiang, Y. Zhang, S. V. Dubonos, I. V. Grigorieva, and A. A. Firsov, Science **306**, 666–669 (2004).
[15]H. Cao, Q. Yu, L. A. Jauregui, J. Tian, W. Wu, Z. Liu, R. Jalilian, D. K. Benjamin, Z. Jiang, J. Bao *et al*., Appl. Phys. Lett. **96**, 122106 (2010).
[16]K. S. Novoselov, A. K. Geim, S. V. Morozov, D. Jiang, M. I. Katsnelson, I. V. Grigorieva, S. V. Dubonos, and A. A. Firsov, Nature **438**, 197–200 (2005).
[17]Y. Dan, Y. Lu, N. J. Kybert, Z. Luo, and A. T. C. Johnson, Nano Lett. **9**, 1472–1475 (2009).
[18]F. Schedin, A. K. Geim, S. V. Morozov, E. W. Hill, P. Blake, M. I. Katsnelson, and K. S. Novoselov, Nat. Mater. **6**, 652–655 (2007)
[19]J. H. Chen, C. Jang, S. Adam, M. S. Fuhrer, E. D. Williams, and M. Ishigami, Nat. Phys. **4**, 377–381 (2008).
[20]M. Lafkioti, B. Krauss, T. Lohmann, U. Zschieschang, H. Klauk, K. v Klitzing, and J. H. Smet, Nano Lett. **10**, 1149–1153 (2012).
[21]R. Wang, S. Wang, D. Zhang, Z. Li, Y. Fang, and X. Qiu, ACS Nano **5**, 408–412 (2011).
[22]W. Hyoung Lee, J. Park, Y. Kim, K. S. Kim, B. H. Hong, and K. Cho, Adv. Mater. **23**, 3460–3464 (2011).
[23]J. Shim, C. H. Lui, T. Yeoung Ko, Y.-J. Yu, P. Kim, T. F. Heinz, and S. Ryu, Nano Lett. **12**, 648–654 (2012).

Downloaded 27 Jun 2012 to 130.91.117.41. Redistribution subject to AIP license or copyright; see http://apl.aip.org/about/rights_and_permissions